Geophys. J. R. astr. Soc. (1975) **43**, 555–572.

A Geophysical Study of the Red Sea Axial Trough between 20·5° and 22°N*

Roger C. Searle and David A. Ross

(Received 1975 January 17)†

Summary

New bathymetric, seismic reflexion, gravity and magnetic data have been obtained in a detailed survey of part of the axial trough in the central Red Sea. These data show that the trough is not continuous, but is broken into two sections separated by a shallow region, called the ' inter-trough zone '. This zone has a thick sediment cover and is devoid of magnetic anomalies. It may represent a fracture zone into which salt and other sediments have flowed, or it may be a section of spreading axis which has remained covered with sediments for an unknown reason.

The transverse magnetic anomalies, previously recognized by Allan, Phillips and other, have been fully mapped, and a further transverse lineation has been discovered. Using three-dimensional computations, a model has been developed which can account for these lineations as the magnetic end-effects of a series of short spreading axes offset by closely-spaced transform faults. The development of such a configuration is discussed and can be seen as a natural consequence of the plate geometry in this region.

Introduction

In March 1971, RV *Chain* spent one month working in the south and central Red Sea. The cruise included a detailed geophysical investigation of the axial trough in the region of Atlantis II Deep, the results of which are reported here.

The Red Sea consists of a wide main trough which is bisected south of 24°N by a deeper axial trough (Drake & Girdler 1964). Seismic refraction measurements (Drake & Girdler 1964; Tramontini & Davies 1969) suggest that much of the main trough is underlain by oceanic lithosphere, and this seems to be confirmed by Girdler & Styles' (1974) observation of marine magnetic anomalies near the western margin of the Red Sea. Several kilometres of Miocene evaporites are found in and near the main trough (Frazier 1970; Ahmed 1972; Lowell & Genik 1972) and were probably deposited during a Miocene spreading hiatus. The top of the evaporite sequence is associated with a prominent acoustic reflector, S, found throughout the main trough (Knott, Bunce & Chase 1966; Phillips & Ross 1970; Ross & Schlee 1973), and the evaporites are overlain by a succession of post-Miocene silts, clays and oozes (Whitmarsh, Weser, Ross *et al.* 1974).

* Contribution No. 3101 of the Woods Hole Oceanographic Institution

† Received in original form 1974 October 10.

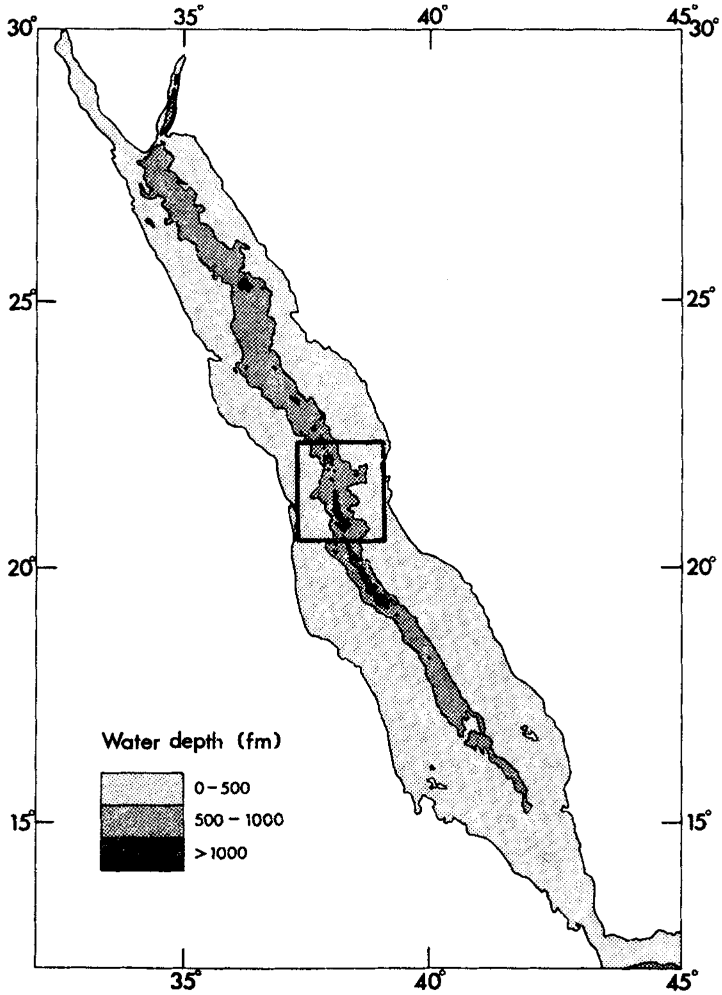

FIG. 1. The Red Sea, showing location of survey. Area of Figs 2, 4 and 6 is indicated by bold rectangle. 500 and 1000 fm (914 and 1829 m) contours from Laughton (1970).

The axial trough is rough-bottomed and generally devoid of thick sediment accumulations; it is seismically active (Fairhead & Girdler 1970) and a region of high heat-flow (Girdler 1970); all this indicates that it is the site of an active spreading axis. No fracture zones have been recognized in the Red Sea, but earthquake focal mechanisms (Sykes 1968; Fairhead & Girdler 1970) and plate tectonic studies (McKenzie, Davies & Molnar 1970; Girdler & Darracott 1972) imply a NE–SW spreading direction. High-amplitude magnetic anomalies over the axial trough are consistent with sea-floor spreading at about 1 cm y^{-1} in this direction for at least the last 2·4 My (Vine 1966; Phillips, Woodside & Bowin 1969; Allan 1970). The absence of reflector S and its underlying sediments from the axial trough confirms that the trough has formed as a consequence of post-Miocene sea-floor spreading (Phillips & Ross 1970), though its width may have been modified in places by salt-flowage (Girdler & Whitmarsh 1974).

The area chosen for our survey (Fig. 1) is of particular interest for two reasons. First, the axial trough is less continuous here than in the south, comprising a number of isolated basins (Figs 1 and 2), separated by relatively shallow, smooth-bottomed areas, one of which has been named an ' inter-trough zone ' by Tramontini & Davies (1969). The basins contain hot brines and metalliferous sediments and, though also found elsewhere in the Red Sea, they are particularly abundant in this area (Degens & Ross 1969; Bäcker & Schoell 1972). Secondly, although the Red Sea magnetic anomalies are normally parallel to the axial trough, Phillips *et al.* (1969), Allan (1970) and Kabbani (1970) found that in this region they strike transverse to the general trend of the Red Sea. One of these transverse lineations was surveyed in some detail by Phillips *et al.* (1969), who concluded that the anomaly was due to a spreading axis striking 070°. Phillips (1970) discussed other models but did not completely resolve the origin of these features. A new hypothesis for the origin of these anomalies is developed later in this paper.

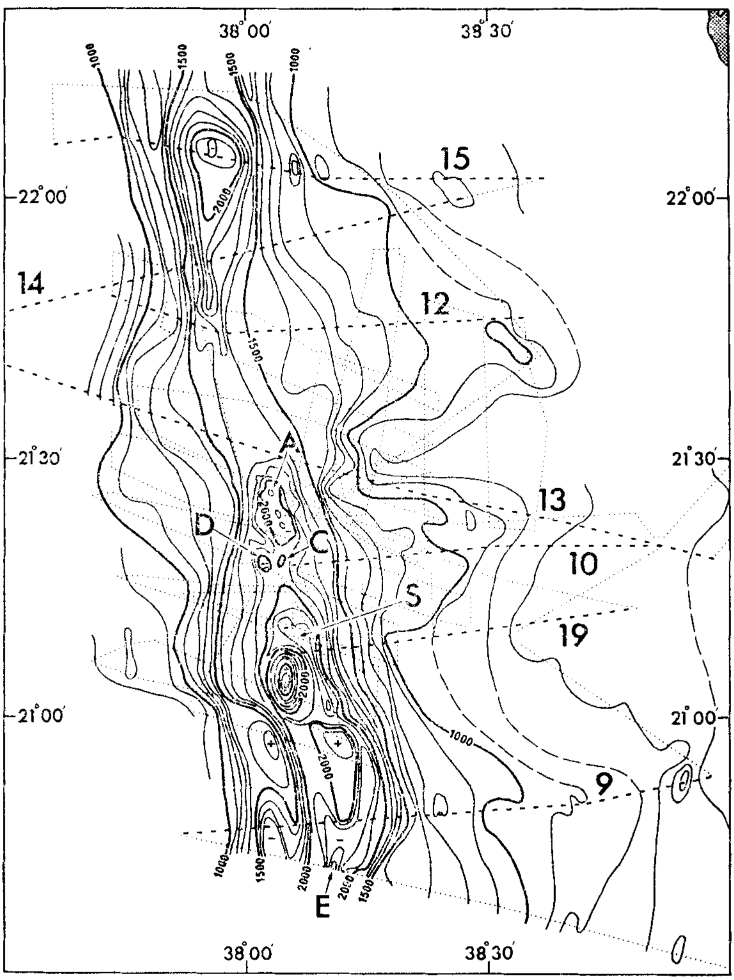

FIG. 2. Bathymetry of the survey area. Contours in corrected metres at 100-m intervals. Ship's track is shown by dotted line, position of reflexion profiles by dashed lines with numbers. A: Atlantis II Deep; C: Chain Deeps; D: Discovery Deep; E: Erba Deep; S: Shagara Deep.

s

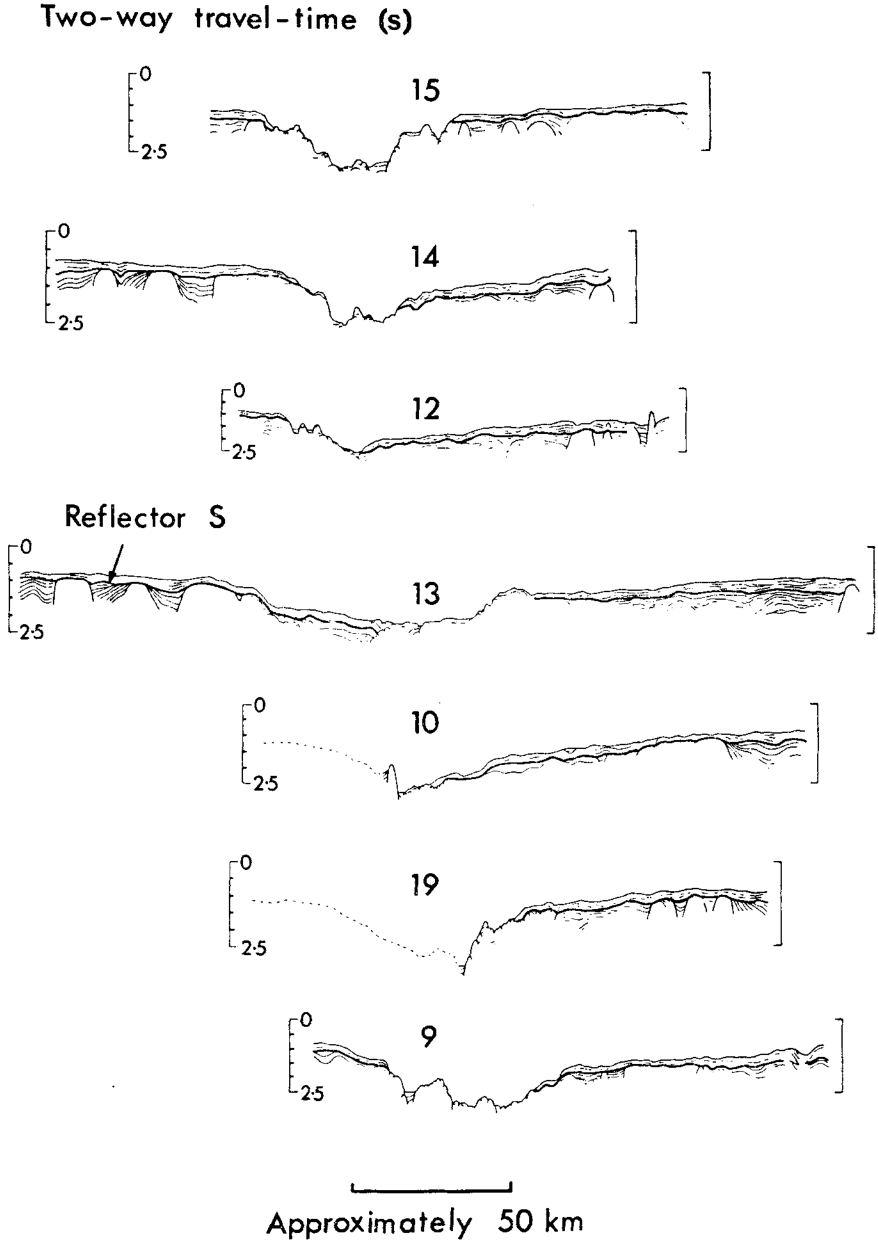

FIG. 3. Line drawings of seismic reflexion profiles over the central Red Sea. For profile positions, see Fig. 2. Profiles have been adjusted to a common mean horizontal scale, but no correction has been made for variations of ship's speed along each profile. The vertical scale varies slightly between profiles. West is to the left on all profiles. Sea-floor west of axial trough in profiles 10 and 19 is shown by broken line based on contours of Fig. 2. Reflector S is indicated by a heavy line.

Bathymetry and seismic reflexion profiles

The track followed by RV *Chain* during our survey is shown in Fig. 2. In most of the survey area, track spacing averaged about 7 km. Navigation was by satellite and celestial fixes, and during part of the survey by radar fixes on an anchored buoy. Depth was measured along all tracks by means of a 3·5 kHz precision echo-sounder. Seismic reflexion profiling was carried out on a number of traverses of the axial trough, using the instrumentation described by Ross & Schlee (1973). The results are presented in Figs 2 and 3.

Norht of 21°45′N, and south of 21°30′N, the axial trough is well developed and is characterized by a deep, rugged floor and steep sides (Fig. 3, profiles 9, 14, 15). We shall refer to these regions as the ' axial trough sections '. Both axial trough sections have rough, but relatively flat, floors, on which are superimposed axial or sub-axial highs which may be analogous to the volcanic ridges discovered in the Mid-Atlantic Ridge axial valley in the FAMOUS area (Needham & Francheteau 1974).

Although the general trend of the axial trough in Fig. 2 is about 350°, detailed surveys (Ross, Hays & Allstrom 1969; Bäcker & Richter 1973) show that the axial trough walls actually strike about 330° in this region, suggesting the existence of dextral offsets between different axial trough sections. One such offset occurs near 21°15′N between Atlantis II and Shagara Deeps, and is clearly shown in Fig. 1 of Bäcker & Richter (1973). Projecting 330° axial trough walls north-west from Atlantis II Deep would bring them west of the actual position of the northern axial trough section, so there must be another dextral offset in this region, possibly associated with the inter-trough zone. We infer that these offsets are due to short transform faults.

Very little sediment is observed within the axial trough sections. Reflector S often outcrops on the sides of the axial trough, but is not observed beneath its floor (Fig. 3, profile 15).

The inter-trough zone is quite different from the axial trough sections. As well as being shallow, its floor is considerably smoother than that of the axial trough sections and its sides are much less steep. Whereas the axial trough sections are often bounded by steep scarps, in the inter-trough zone the sea-floor slopes gently down toward the deepest part. (Because of its obliquity, profile 13, which crosses part of the inter-trough zone, does not show this clearly—in fact the steep slopes seen on this profile belong to the axial trough sections to the north and south. The eastern part of profile 12 presents a clearer illustration of the gently sloping side of the inter-trough zone.) Profile 10, whose west end crosses the offset south of Atlantis II Deep shows a similar gradual descent to the deepest point.

Thick sediments do occur within the inter-trough zone. The eastern part of profile 12, and the western part of 13, which cross the inter-trough zone, clearly show reflector S and the overlying sediments continuing right up to the axis of the Red Sea. On profile 13 the layered reflectors which are typical of the Miocene sediments beneath S can also be clearly seen near the centre. Acoustic basement was not reached, but the total thickness of sediments near the centre is greater than 0·9 s, equivalent to about 800 m. There is thus a strong implication that the sediment and evaporite sequences are continuous across the inter-trough zone. (The rough-bottomed section of profile 12 and the smoother, though acoustically opaque, section of profile 13 probably represent the ends of the axial trough sections.) In the region of profile 10 (incidently very close to the Deep Sea Drilling Project site 227) the uppermost sediments and reflector S also continue almost to the axis of the Sea.

Gravity

Gravity was measured south of 21°55′N using a vibrating string gravimeter

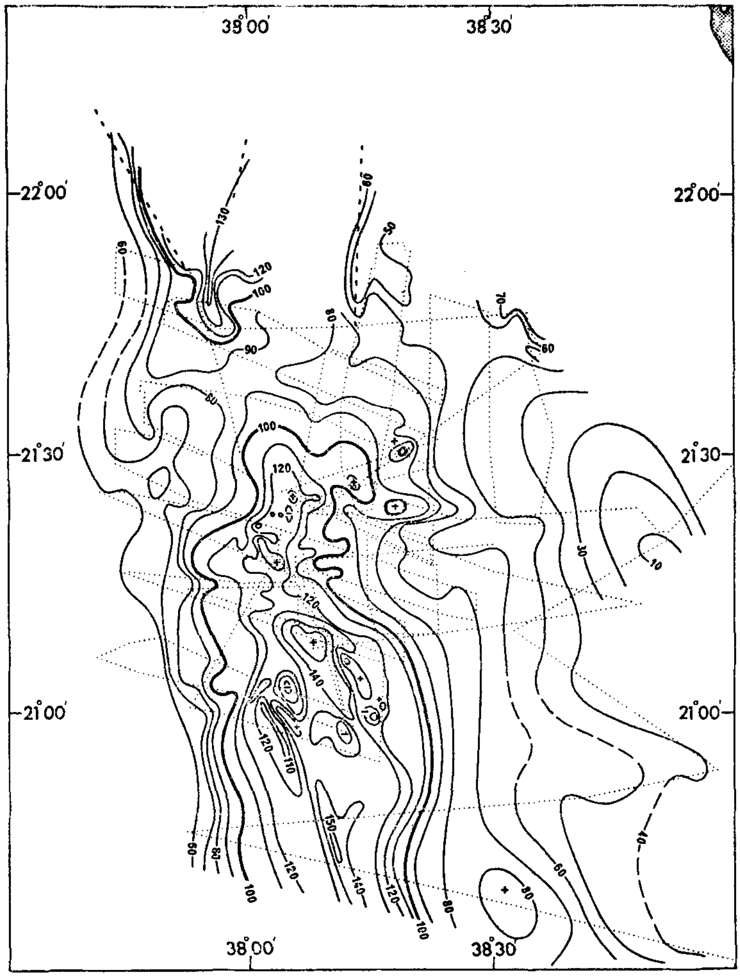

FIG. 4. Contoured chart of simple Bouguer anomalies over the survey area, in milligals. Track of *Chain* cruise 100 (March 1971) is shown by dotted line. Dashed lines in north represent tracks of other cruises from which data were taken.

similar to the system described by Bowin, Aldrich & Folinsbee (1972), and data from other cruises were used to supplement our measurements in the north.

Fig. 4 is a chart of the Bouguer anomaly over the survey area, contoured at 10-mgal intervals. The average cross-over error is about 5 mgal. The Bouguer correction which has been applied is the calculated attraction of an infinite horizontal slab, of thickness equal to the water depth below the observation point and density (2·67–1·03)g cm^{-3}. The maximum error due to these simplifying assumptions is an over-estimation of the amplitude of the anomaly over the axial trough, compared with that over the main trough, by about 10 mgal. The error in relative magnitudes of anomalies over different parts of the axial trough will be much less. These effects are small compared to the observed variations in anomaly amplitude.

The well-known positive anomaly over the axial trough is clearly seen in Fig. 4. However, its amplitude is much reduced over the inter-trough zone, where it reaches a mean maximum of around 90 mgal, compared with about 120 mgal over Atlantis II Deep and 140 mgal farther south.

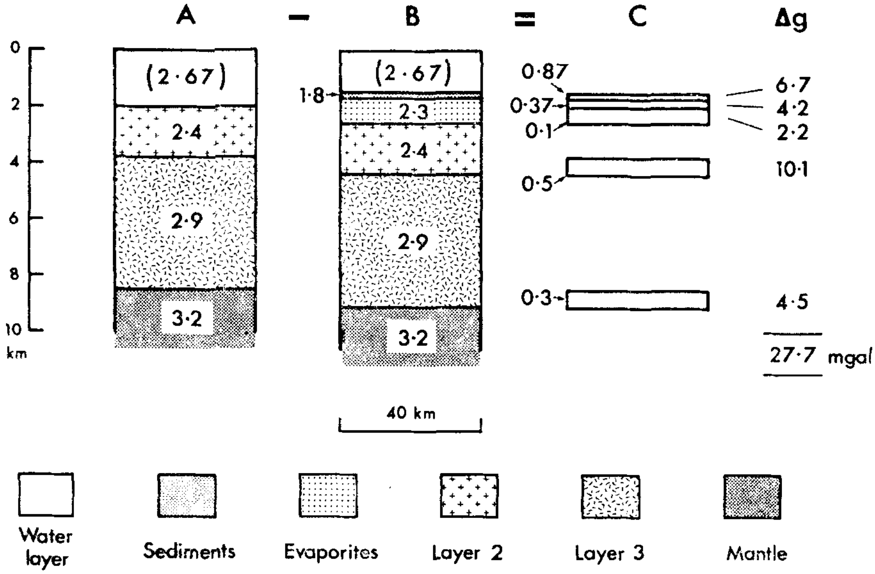

FIG. 5. Schematic diagram of gravity interpretation. A, assumed crustal structure in Atlantis II Deep area. Numbers in crustal section are specific gravities. A value of 2·67 is used in the uppermost layer because in calculating Bouguer anomalies the water has been 'replaced' by rock of this density. B, possible structure for the inter-trough zone. As A, except for sediments and evaporites on top of layer 2 which have depressed lithosphere by 600 m. C, density contrasts between A and B. The lateral extent of these differences should be about 40 km, the width of inter-trough zone. The density contrasts then give rise to the gravity anomalies indicated in the right-hand column.

Calculations show that this difference in gravity can be completely explained by the presence of the sediments and the lithosphere's isostatic response to them. About one kilometre of sediments beneath the inter-trough zone, combined with the depression of the basement by several hundred metres which would be required to maintain isostatic equilibrium, produces a Bouguer anomaly of about -28 mgal relative to Atlantis II Deep (Fig. 5). The amount of isostatic adjustment and the inferred sediment thickness depend on the densities assumed for the sediments and substratum, but the gravity anomaly is rather insensitive to these assumptions. For example, increasing the sediment density causes deeper sinking of the lithosphere and therefore a greater inferred sediment thickness, but it also renders the near-surface density contrast less negative, and these two effects almost cancel each other out. This interpretation is consistent with the seismic refraction results of Tramontini & Davies (1969) which showed that layer 3 is deeper under their inter-trough zone than under the normal axial trough.

Of course this simple-minded interpretation is not unique, but we consider it significant that the observed differences in depth and gravity between the inter-trough zone and the axial trough sections can be so simply explained in terms of the observed sediment distribution. There is therefore no need to assume any major differences in lithospheric structure at depth. We shall consider in a later section how the required sediment thickness could have been deposited so close to the Red Sea axis.

Magnetic anomalies

Fig. 6 is the total-field magnetic anomaly chart of the survey area, with the indi-

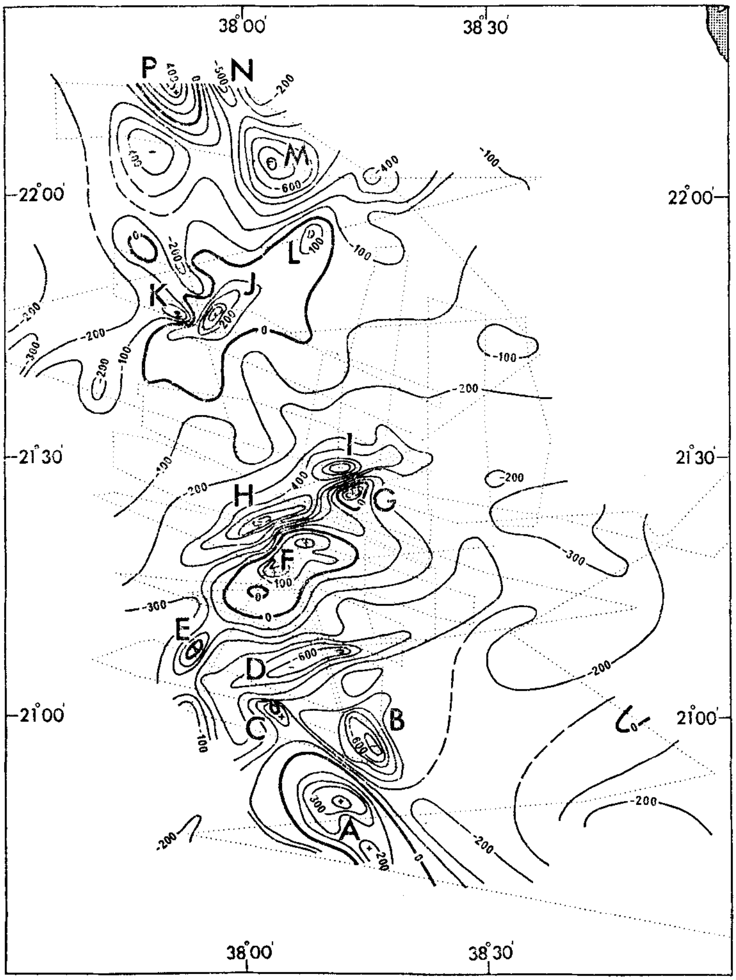

FIG. 6. Total field magnetic anomalies over survey area, in nT (gammas). Ship's track shown by dotted lines. Anomalies have been lettered for ease of reference.

vidual anomalies lettered for reference. Data were acquired using a towed proton precession magnetometer, and reduced by removal of the International Geomagnetic Reference Field (IAGA Commission 2 Working Group 4, 1969). (The average value of the reduced field is about −200 nT (gamma), indicating that the IGRF is too high in this region.) No correction was made for daily variation. Our main objective was to study the relationship between the transverse magnetic anomalies (strike 070°) and the more widespread 330° magnetic and bathymetric trends found elsewhere in the Red Sea. Ship's track was therefore oriented ESE–WNW to bisect the angle between these trends and thus to minimize directional bias in the contouring of the anomalies.

Large-amplitude magnetic anomalies were found only near the axial trough sections, although the axial trough itself is slightly narrower than the region of high magnetic relief, possibly as a result of lateral salt-flowage. In contrast, the inter-trough zone is completely devoid of major magnetic anomalies.

Within the area of Fig. 6, only the anomalies A, B and possibly M, N and P (in the extreme south and north) strike parallel to the Red Sea axis. All the other magnetic lineations are transverse to this trend, striking between 050° and 070°. The pair of lineations *EFG* and *HI* are those previously described by Phillips *et al.* (1969) and Kabbani (1970). We have found a third transverse anomaly, *D*, and possibly a fourth, *JL*, although the contouring of the latter is rather uncertain because of the wider track-spacing employed in the north.

Most linear magnetic anomalies over the ocean floor are formed at mid-ocean ridges and are parallel to spreading axes (Vine & Matthews 1963). However, magnetic anomalies are also sometimes found associated with and roughly parallel to fracture zones (Mason & Raff 1961; Malahoff & Woollard 1968, 1970; Rea 1972; Vogt, Anderson & Bracey 1971; Cochran 1973; Klitgord *et al.* 1974; Schouten 1974; Collette *et al.* 1974). In the latter case they may be due to magnetized material intruded along a fracture zone which has opened due to thermal contraction (Turcotte 1974) or which represents a leaky transform fault, or more simply they may be due to the magnetic end-effects of the Vine–Matthews blocks.

In the area of our survey, which is about 12° north of the magnetic equator and has low magnetic declination, the major contribution to magnetic anomalies comes from north- or south-facing edges of magnetized bodies. East- or west-facing edges produce only very small anomalies here. This is also clearly brought out in Schouten's (1971) spectral analysis of marine magnetic profiles. Collette *et al.* (1974) have discussed the formation of E–W striking magnetic anomalies over fracture zones, using the technique of ' reduction to the pole ' (Schouten & McCamy 1972) to remove the asymmetry of the observed profile. However, that technique is essentially two-dimensional; to interpret our detailed survey we considered a three-dimensional approach more appropriate.

The northern and southern faces of normally magnetized blocks give rise to negative and positive anomalies, respectively; for reversely magnetized bodies, the signs are reversed. Thus, a normally magnetized body (say, the block of sea floor produced during the Brunhes epoch) striking NW–SE would have a negative anomaly along its north-east side *and* over its northern end, and a positive anomaly on its south-west side and southern end. The transverse anomalies in the Red Sea may thus be generated at the sides of Vine–Matthews blocks striking NE–SW (transverse spreading axis model), the sides of bodies intruded along NE–SW transform faults (leaky transform fault model), or the ends of NNW–SSE trending Vine–Matthews blocks (magnetic end-effect model). We shall examine these three possibilities in turn.

Transverse spreading-axis models

If there is a spreading axis striking NE–SW in the central Red Sea, it must be joined to other segments of spreading axis (with the same or different trend) either directly or by transform faults. Fig. 7(a) (b), (d) and (e) represent the most plausible ways of doing this. A model similar to Fig. 7(d) was discussed by Phillips *et al.* (1969) and Phillips (1970) considered a model like Fig. 7(a).

In order to produce the observed anomalies the transverse spreading axis segment would have to be some 30 km long and strike 060°. In the case of model Fig. 7(a), this would offset the two NNW-striking segments by a much larger amount than is indicated by the bathymetry (Fig. 2). Moreover we observe no NNW-striking anomalies north of the eastern end of the transverse segment, as would be predicted by the model. Such anomalies would not be seen if the northernmost segment of spreading axis had a very northerly strike, but such a configuration would make the agreement with the bathymetry even worse.

In model Fig. 7(b), the southernmost transform fault would lie between the northern ends of magnetic anomalies *B* and *C*, and the western ends of *F* and *H* (Fig. 6). This implies a NW–SE spreading direction, which is quite inconsistent with the

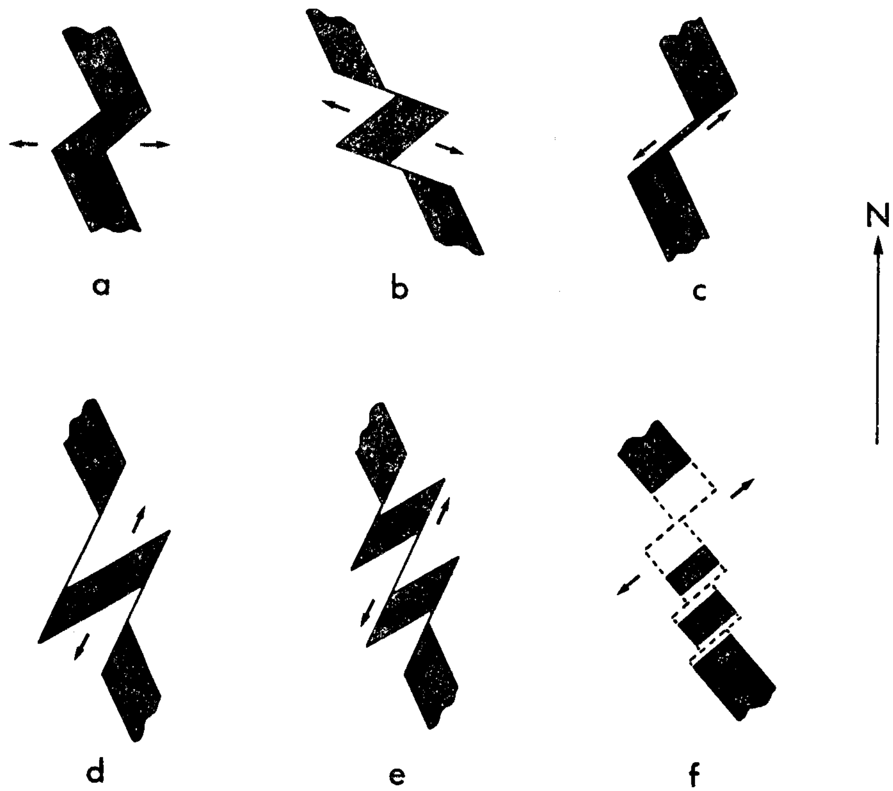

FIG. 7. Possible spreading schemes in the central Red Sea. Arrows give spreading direction, sea floor with strong Brunhes magnetization shown in black. For further explanation see text.

observed earthquake mechanisms (Sykes 1968; Fairhead & Girdler 1970) and the plate-tectonic interpretations of the Red Sea (McKenzie *et al.* 1970; Girdler & Darracott 1972), which indicate roughly NE–SW spreading directions.

The model shown in Fig. 7(d) has the transforms striking approximately NE, and Fig. 7(e) is similar except that a second transverse spreading axis has been added to account for the possible northern transverse anomalies *JL*. These models are both reasonably consistent with the observed anomalies and the required spreading direction. An earlier version of Fig. 7(d) required an almost N–S spreading direction (Phillips 1970), but this can be modified to 020° or 030° by allowing the transform faults to be associated with non-magnetic zones of finite width. One objection to these models is that they require a highly acute angle between spreading axis and transform fault. Such a disposition is unlikely on physical and intuitive grounds (Lachenbruch & Thompson 1972), and is unknown elsewhere; indeed where the orthogonality of ridges to transform faults is upset by changes of spreading direction, the ridges usually realign themselves perpendicular to the transforms within a few million years (Menard & Atwater 1968). However, the main objection to these models is that they are not in good agreement with the observed bathymetry. Detailed investigations of the Atlantis II Deep region by Bäcker & Richter (1973) show that the major bathymetric trends in the region of the transverse anomalies strike 330°, a direction which is not represented in the parts of these models supposed to produce the transverse anomalies.

Finally, all the models in this category fail to account adequately for anomaly *D*. Qualitatively it can be explained as an end-effect of a NW trending spreading axis to the south, but calculations show that the observed shape and amplitude of the anomaly are not well reproduced by models of this geometry.

Leaky transform-fault model

Phillips (1970) has discussed a model similar to that shown in Fig. 7(c), in which the transverse anomalies were considered to represent the trace of a transform fault. One explanation of magnetic anomalies along such faults is that the transform has become ' leaky ' and magnetized material has been intruded along it (e.g. Malahoff & Woollard 1970; Rea 1972).

If the offset along the transform is fairly large, then recent normally magnetised material intruded along it might be adjacent to older reversely magnetized sea floor on either side, producing anomalies similar to those observed. However, this case is essentially similar to model Fig. 7 (a), and the same objections apply. The large offset required cannot occur in the Atlantis II Deep region, and over most of the area covered by anomalies *F* and *H*, even assuming a transform fault were present, the sea floor on either side of it would be normally magnetized. In that case, the only way of producing the transverse lineations would be to assume that intrusions along the transform had a much higher intensity of magnetization than the normal sea floor of Brunhes age. We consider such an assumption unjustified since the transverse anomalies can be more simply interpreted in terms of magnetic end-effects. A further objection to the leaky-transform hypothesis is that, to reproduce anomalies *F* and *H*, it would be necessary for the transform to pass through the Atlantis II Deep. However, the observed morphology and pattern of hydrothermal activity in the Deep suggest it is part of a NNW trending spreading axis (Bäcker & Richter 1973), while the bathymetry contains no evidence of offsets in the flanking scarps corresponding to the expected position of the fault.

Magnetic end-effect model

The third possibility is that the transverse lineations are generated over the north and south ends of Vine–Matthews blocks striking NNW–SSE, parallel to the general trend of the Red Sea (Fig. 7(f)). If a number of relatively short segments of spreading axis are offset along small transform faults, the observed transverse lineations can be reproduced quite well, providing the transform faults are associated with zones of very low, possibly zero, intensity of magnetization. It is then the magnetization contrast between the ordinarily magnetic sea-floor and the non-magnetic zone which produces the transverse lineations.

Non-magnetic areas several tens of kilometres wide are associated with many fracture zones (Mason & Raff 1961; Matthews, Vine & Cann 1965; Bergh 1971; Cochran 1973; Schouten 1974; Collette *et al.* 1974), and in some cases can give rise to magnetic anomalies parallel to the fractures without the need to assume additional intrusion of magnetized material along them. The existence of such a zone does not of course mean that no sea-floor spreading has taken place there; it merely means that the new lithosphere produced within that zone has a very low intensity of magnetization. A number of mechanisms may be thought of to cause this. Matthews *et al.* (1965) suggested that fracture zones could have low magnetization as a result of the destruction of coherently-magnetized bodies by intense brecciation, perhaps accompanied by hydro-thermal alteration. Secondly, if a transform fault is leaky, the intrusive zone may be so narrow that the intrusions along it are effectively randomly distributed with respect to magnetic polarity, thus producing a low net magnetization.

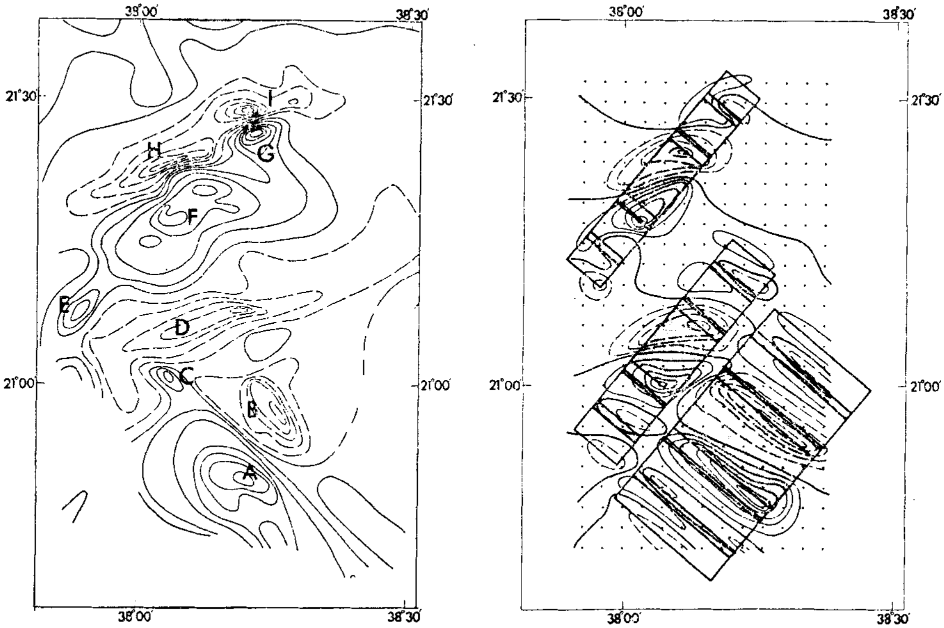

FIG. 8. (a): Observed magnetic anomalies—detail from southern part of Fig. 6. Contours of less than −200 nT are represented by broken lines. (b) Model and computed anomalies. Stippled areas represent normally magnetized sea-floor, white areas within heavy lines, reversely magnetized sea-floor. Other areas, zero magnetization. The model assumes spreading at 1 cm yr^{-1} in a 040° direction and the time scale of Heirtzler *et al.* (1968). The magnetized bodies are 200 m thick and have intensities of magnetization of 40 Am^{-1} in the central blocks and 20 Am^{-1} elsewhere. Tops of bodies are at depths of 2·4 km below sea-level for the northernmost zone and 2·6 km for the other two zones. Magnetic anomaly was computed for each point on the grid (dots) and contoured at 100-nT intervals. Heavy line, 0 nT. Continuous lines, positive anomalies. Broken lines, negative anomalies.

Another possibility in the central Red Sea, where we have seen that thick sediments are found near the axis in the region of offsets of the axial trough, is that the basalts were intruded into sediments rather than extruded on the sea floor. Because intrusions cool slowly, they have a larger grain-size which results in a much lower remanent magnetization (Irving 1970). Finally, we may speculate that the mineralogy of fracture-zone basalts could be sufficiently different from that of ridge basalts to render the magnetization of the former very low.

We have computed the anomalies produced by several models such as Fig. 7(f). For this purpose, a program written and kindly supplied to one of us (RCS) by M. Talwani was modified to compute the anomaly due to a three-dimensional model comprising a number of separate bodies with differing magnetizations. Fig. 8(b) shows one of the models we consider to be a successful fit to the observations. Fig. 8(a) is an enlarged section of Fig. 6, at the same scale, for comparison. Because of the poorer observational control in the north, no attempt was made to model anomalies north of the inter-trough zone.

This model successfully predicts all of the major high-amplitude anomalies observed, with the exception of *E*, *G*, and *I*. *G* and *I* are typical of the anomalies which would be produced by a simple dipole source, and might be due to an isolated intrusion or buried sea-mount. It can be seen that the transverse anomalies produced by the model are longer than the width of the Brunhes blocks for two reasons: first because both the ends and the sides of these blocks contribute to the anomalies, and secondly because the opposite ends of the adjacent reversed (Matuyama) blocks contribute to the same lineation. Induced magnetization has been ignored in these models, but if a component of induced magnetization is assumed in the magnetized zones, then the transverse anomalies can be somewhat extended in the spreading direction, corresponding for example to the ENE extension of the $-300\,\gamma$ contour round anomaly *D*. Some details of the anomaly shapes, for example the slight curve of the lineations and the slightly different trends of lineations *F* and *H*, are reproduced by the model. These features are only apparent as a result of the use of three-dimensional modelling.

The model generates a set of anomalies 1·8-My old (anomaly 2) outside the axial trough which we do not in fact observe. This may be becasue the older source-bodies are deeper than we have assumed, perhaps due to sinking under the sediment overburden; or because at that time low magnetizations resulted from predominantly intrusive magmatism beneath residual evaporite deposits at the spreading axis.

Note that the anomalies predicted by the model do not strike parallel to the transform faults. This occurs because the magnetized blocks have widths comparable to their lengths. As a consequence, one cannot *accurately* determine the spreading direction from the magnetic anomaly directions. Models similar to that in Fig. 8(b) but with different spreading directions were also constructed. Any similar model with a spreading direction between about 030° and 050° can fit the data almost as well, and would not provide any serious conflict with the plate tectonics of the region. In fact the trends of anomalies *A* and *B* and of the marginal scarps of the axial trough suggest that the spreading axes might strike as northerly as 320° or 330° rather than the 310° of our model. However, a model with a transform fault direction of 050° or more does not reproduce the transverse lineations so well. Possibly this discrepancy should be resolved by allowing slightly oblique spreading, i.e. with spreading axes striking 320° to 330° and transform faults striking 040°.

The model is also consistent with the bathymetry. The positions of the Brunhes blocks generally coincide with the deep water of the axial trough, and the observed and modelled offsets also correspond. The gap between the two northernmost magnetized zones in the model corresponds to the position of the transform fault inferred south of Atlantis II Deep. The gap between the southern two magnetized zones of the model has little expression in the bathymetry and it is in fact possible to model the anomalies reasonably well if these zones are joined by short north–south trending magnetized blocks. This would also reproduce better the shape of anomaly *C*. However, the small dextral offset must remain in order to separate anomaly *A* from *C* and *B* from *D* as observed.

The nature of the inter-trough zone

It is necessary to account for the shallowness, sediment cover, and lack of magnetic anomalies in the inter-trough zone in a way which is consistant both with our interpretation of the region immediately to the south, and with the regional plate-tectonics. There seem to be two possibilities: either this is a section of spreading axis (joined to the axial trough sections to north and south by transform faults) where the overlying sediments have been thinned but not yet rifted apart, or it is part of a wide fracture zone infilled with sediments in a similar way to the smaller offset zone south of Atlantis II Deep. If it is a spreading axis, then the lack of magnetic anomalies should probably be attributed to the fact that its basalts have been intruded into sediments and thus have a low remanent magnetization. However, it is difficult to understand why thick sediments should have remained over a section of spreading axis here when those from adjacent axial trough sections have been rifted apart.

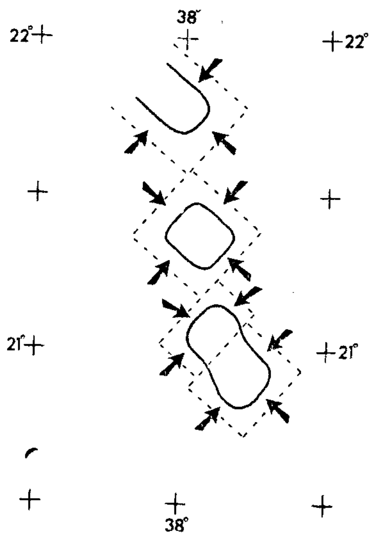

FIG. 9. Sketch to indicate how salt flowage (arrows) could account for approximate present distribution of sediments. Sediment-free areas are outlined by full lines. Broken lines represent possible approximate boundary of 1·5-My-old sea-floor, as deduced from model.

This can be understood if the inter-trough zone is not a simple spreading centre but part of a wide fracture zone which pre-dated the period of post-Miocene salt flowage. Such a fracture zone, if characterised by a large transverse trough, would have offered a preferred path by which flowing salt could reach deep into the newly forming axial valley. The disposition of the 500-fm contours on either side of the inter-trough zone, and also near 20°30′N (Fig. 1) are indeed suggestive of the presence of partially filled transverse troughs. The width of the inter-trough zone is about 25 km, which is comparable with other large fracture zones. Even in the absence of such a trough, the offset associated with a transform fault across the inter-trough zone would facilitate salt flowage as shown in Fig. 9. It is clear from this figure that where an appreciable offset occurs (e.g. across the inter-trough zone and south of Atlantis II Deep), salt can flow into the axial trough sections from their ends as well as their sides. In this case, the lack of magnetic anomalies over the inter-trough zone might be due to any of the mechanisms suggested earlier for the production of non-magnetic rocks in fracture zones.

Development of the inferred structures

We have presented a model of the geological structure of the central Red Sea which is characterised by a number of short spreading-centres offset by closely-spaced transform faults. Our observations give no indication of the structure prior to about 1·8 My BP, but the ideas of Menard & Atwater (1968) can be used to suggest how the present configuration of the plate boundary may have developed (Fig. 10). At the onset of spreading the initial fracture, whose strike is suggested by the present trend of the coast lines, would have been almost due north between 20·5°N and 22°N (Fig. 10(a)). Thus the initial spreading axis here would have lain at an oblique angle to the NE–SW spreading direction. In such a situation the spreading axis would be expected to break up into a number of shorter sections joined by orthogonal transform faults (Fig. 10(b)) which would subsequently develop as shown in Fig. 10(c)–(d).

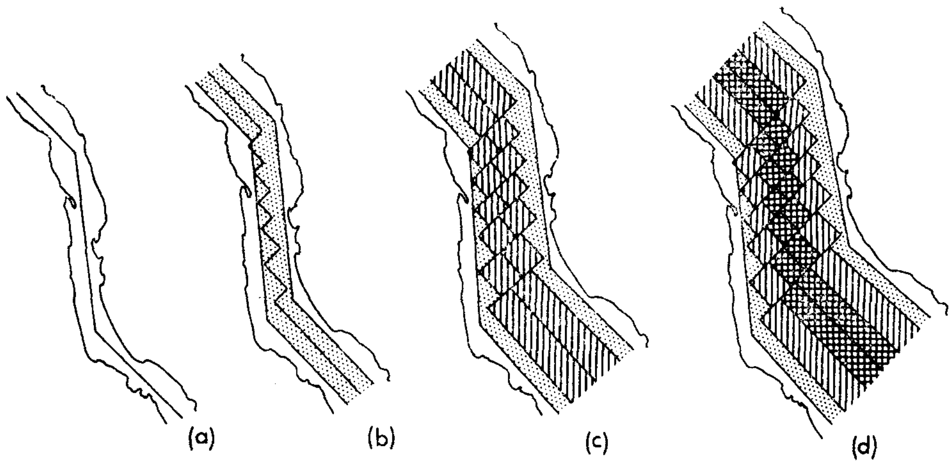

FIG. 10. Sketch to illustrate how the inferred pattern of closely-spaced transform faults could have developed in the central Red Sea. The sketch is not intended to represent an accurate reconstruction: in particular, the boundaries between shadings do not necessarily represent equally-spaced isochrons, and the existence and positions of some transform faults are conjectural.

We have no evidence with which to date the formation of these transform faults, but we suspect it would have occurred soon after the initial onset of sea-floor spreading, since oblique spreading seems to be inherently unstable.

Because of the offsets effected by the transform faults, salt could easily flow into the axial trough, dividing it into a number of short sections surrounded on all four sides by evaporite outcrops (Fig. 9). On the basis of coincidences in the levels of the free brine surfaces and outcrops of reflector S, it has been suggested that the brines may have been derived from the evaporites by leaching (Whitmarsh, Weser, Ross *et al.* 1974, p. 600). Clearly the structure indicated in Fig. 9 would facilitate such a process. To the north of this region the angle between spreading direction and the Red Sea axis becomes increasingly acute (Girdler & Darracott 1972) implying the presence of more closely-spaced transforms and therefore more brines, which do indeed occur (Bäcker & Schoell 1972). However, there are few brines to the south where the spreading direction is almost perpendicular to the axis so that fewer transforms are to be expected.

The occurrence of transverse magnetic lineations, sedimented areas on the axis of the Red Sea, and numerous dense brines within the central part of the Red Sea can thus be seen to be natural consequences of the plate geometry.

Transverse anomalies elsewhere

Our three-dimensional calculations have shown that, in regions where fracture zones are closely spaced, the magnetic lineation pattern produced may be quite unexpected and, in particular, lineations parallel to spreading axes may be weak or absent. We would therefore recommend that in other similar areas three-dimensional modelling might be of value in understanding the magnetic pattern. One possible example is the Gulf of California, where the major magnetic lineations parallel the transform faults, and any anomalies over the spreading axes are very weak (Hilde 1964; Larson *et al.* 1972; Klitgord *et al.* 1974).

Acknowledgments

Data presented here were collected during Cruise 100 of RV *Chain*, which was sponsored by the United States Geological Survey and the Ministry of Petroleum and Mineral Resources of the Kingdom of Saudi Arabia. Some of the interpretation was financed by the Natural Environment Research Council. One of us (RCS) was employed at the Geophysical Observatory, University of Addis Ababa during part of the work.

J. D. Phillips and C. O. Bowin of Woods Hole Oceanographic Institution reduced and kindly made available the magnetic and gravity data used here. M. Talwani provided a program for computing magnetic anomalies of three-dimensional bodies. The idea of using short sections of spreading axis to model the magnetics arose during a discussion between RCS and D. G. Roberts. We are also grateful for discussions with R. W. Girdler, S. Hall, J. D. Phillips, J. Schlee, and P. Styles, and we also thank J. C. Behrendt, J. R. Heirtzler, A. S. Laughton and R. B. Whitmarsh for manuscript reviews.

Finally, we wish to express our thanks to the officers and crew of RV *Chain* and to our other colleagues on board for their co-operation during the survey.

R. C. Searle:
Institute of Oceanographic Sciences,
*Wormley, Godalming, Surrey GU*8 5*UB.*

D. A. Ross:
Woods Hole Oceanographic Institution,
Woods Hole, Massachusetts 02543.

References

Ahmed, S. S., 1972. Geology and petroleum prospects in Eastern Red Sea, *Am. Assoc. Petrol. Geol. Bull.*, **56,** (4), 707–719.

Allan, T. D., 1966. A bathymetric chart of the Red Sea, *International Hydrogr. Rev.*, **43,** 33–36.

Allan, T. D., 1970. Magnetic and gravity fields over the Red Sea, *Phil. Trans. R. Soc. Lond.*, **A267,** 153–180.

Bäcker, H. & Richter, H., 1973. Die rezente hydrothermal-sedimentäre Lagerstätte Atlantis-II-Tief im Roten Meer, *Geologische Rundschau*, **62,** 697–741.

Bäcker, H. & Schoell, M., 1972. New Deeps with brines and Metalliferous Sediments in the Red Sea, *Nature Phys. Sci.*, **240,** 153–158.

Bergh, H. W., 1971. Sea-floor spreading in the southwest Indian Ocean, *J. geophys. Res.*, **76,** 6276–6282.

Bowin, C., Aldrich, T. C. & Folinsbee, R. A., 1972. VSA gravitymeter system: tests and recent developments, *J. geophys. Res.*, **77,** 2018–2033.

Cochran, J. R., 1973. Gravity and Magnetic Investigations in the Guiana Basin, Western Equatorial Atlantic, *Geol. Soc. Amer. Bull.*, **84,** (10), 3249–3267.

Collette, B. J., Schouten, H., Rutten, K. & Slootweg, A. P., 1974. Structure of the Mid-Atlantic Ridge province between 12°N and 18°N, *Marine Geophys. Res.*, **2,** (2), 143–179.

Degens, E. T. & Ross, D. A., eds., 1969. *Hot Brines and Heavy Metal Deposits in the Red Sea*, Springer, New York, 600 pp.

Drake, C. L. & Girdler, R. W., 1964. A geophysical study of the Red Sea, *Geophys. J. R. astr. Soc.*, **8,** 473–495.

Fairhead, J. D. & Girdler, R. W., 1970. The seismicity of the Red Sea, Gulf of Aden and Afar Triangle, *Phil. Trans. R. Soc. Lond.*, **A267,** 49–74.

Frazier, S. B., 1970. Adjacent structures of Ethiopia: that portion of the Red Sea coast including Dahlak Kebir Island and Gulf of Zula, *Phil. Trans. R. Soc. Lond.*, **A267,** 131–141.

Girdler, R. W., 1970. A review of Red Sea heat flow, *Phil. Trans. R. Soc. Lond.*, **A267,** 191–203.

Girdler, R. W. & Darracott, B. W., 1972. African Poles of Rotation, *Comment. Earth Sci: Geophys.*, **2,** 131–138.

Girdler, R. W. & Styles, P., 1974. Two stage Red Sea floor spreading, *Nature*, **247,** 7–11.

Girdler, R. W. & Whitmarsh, R. B., 1974. Miocene evaporites in Red Sea cores, their relevance to the problem of the width and age of oceanic crust beneath the Red Sea, in Whitmarsh, R. B., Weser, O. E., Ross. D. A. *et al. Initial Reports of the Deep Sea Drilling Project*, Volume **23,** pp 913–921, Washington (U.S. Government Printing Office).

Heirtzler, J. R., Dickson, G. O., Herron, E. M., Pitman, W. C. & Le Pichon, X., 1968 Marine magnetic anomalies, geomagnetic field reversals, and motions of the ocean floor and continents, *J. geophys. Res.*, **73,** 2119–2136.

Hilde, T. W. C., 1964. Magnetic anomalies across Gulf of California, in: *Marine Geology of the Gulf of California*, eds Tj. H. Van Andel & G. G. Shor, *Am. Assoc. Petr. Geol. Mem.*, **3,** 122–125.

IAGA Commission 2 Working Group 4, 1969. International Geomagnetic Reference Field 1965.0, *J. geophys. Res.*, **74,** 4407–4408.

Irving, E., 1970. The Mid-Atlantic Ridge at 45°N. XIV. Oxidation and magnetic properties of basalt; review and discussion, *Can. J. Earth Sci.*, **7,** 1528–1538.

Kabbani, F. K., 1970. Geophysical and structural aspects of the central Red Sea rift valley, *Phil. Trans. R. Soc. Lond.*, **A267,** 89–97.

Klitgord, K. D., Mudie, J. D., Bischoff, J. L. & Henyey, T. L., 1974. Magnetic anomalies in the Northern and Central Gulf of California, *Geol. Soc. Amer. Bull.*, **85,** (5), 815–820.

Knott, S. T., Bunce, E. T. & Chase, R. L., 1966. Red Sea seismic reflection studies, in: *The World Rift System*, ed. T. N. Irving, Geol. Surv. Canada spec. paper 66–14, 33–61.

Lachenbruch, A. H. & Thompson, G. A., 1972. Oceanic ridges and transform faults: their intersection angles and resistance to plate motions, *Earth Planet. Sci., Lett.*, **15.** 116–122.

Larson, P. A., Mudie, J. D. & Larson, R. L., 1972. Magnetic anomalies and fracture zone trends in the Gulf of California, *Geol. Soc. Am. Bull.*, **83,** (11), 3361–3368.

Laughton, A. S., 1970. A new Bathymetric chart of the Red Sea, *Phil. Trans. R. Soc. Lond.*, **A267,** 21–22.

Lowell, J. D. & Genik, G. J., 1972. Sea-floor spreading and structural evolution of southern Red Sea, *Am. Assoc. Petrol. Geol. Bull.*, **56,** (2), 247–259.

Malahoff, A. & Woollard, G. P., 1968. Magnetic and tectonic trends over Hawaiian Ridge, in: *The Crust and Upper Mantle of the Pacific Area*, eds L. Knopoff, C. L. Drake & P. J. Hart, *A.G.U. Geophys. Mon.* **12,** 241–276.

Malahoff, A. & Woollard, G. P., 1970. Geophysical studies of the Hawaiian Ridge and Murray Fracture Zone, *The Sea*, **4,** part II, 73–131, ed. A. E. Maxwell, Wiley.

Mason, R. G. & Raff, A. D., 1961. Magnetic survey off the west coast of North America, 32°N latitude to 42°N latitude, *Geol. Soc. Am. Bull.*, **72,** 1259–1266.

Matthews, D. H., Vine, F. J. & Cann, J. R., 1965. Geology of an area of the Carlsberg Ridge, Indian Ocean, *Geol. Soc. Am. Bull.*, **76,** 675–682.

McKenzie, D. P., Davies, D. & Molnar, P., 1970. Plate tectonics of the Red Sea and East Africa, *Nature*, **226,** 243–248.

Menard, H. W. & Atwater, T., 1968. Changes in direction of sea floor spreading, *Nature*, **219,** (5153), 463–467.

Needham, H. D. & Francheteau, J., 1974. Some characteristics of the rift valley in the Atlantic Ocean near 36°48′N, *Earth Planet. Sci. Lett.*, **22,** 29–43.

Phillips, J. D., 1970. Magnetic anomalies in the Red Sea, *Phil. Trans. R. Soc. Lond.*, **A267,** 205–217.

Phillips, J. D. & Ross, D. A., 1970. Continuous seismic reflection profiles in the Red Sea, *Phil. Trans. R. Soc. Lond.*, **A267,** 143–152.

Phillips, J. D., Woodside, J. & Bowin, C. O., 1969. Magnetic and gravity anomalies in the central Red Sea, *Hot Brines and Heavy Metal Deposits in the Red Sea*, 98–113, eds E. T. Degens & D. A. Ross, Springer, New York.

Rea, D. K., 1972. Magnetic anomalies along fracture zones, *Nature Phys. Sci.*, **236,** 58–59.

Ross, D. A., Hays, E. E. & Allstrom, F. C., 1969. Bathymetry and continuous seismic profiles of the hot brine region of the Red Sea, *Hot brines and heavy metal deposits in the Red Sea*, 82–97, eds E. T. Degens & D. A. Ross, Springer, New York.

Ross, D. A. & Schlee, J., 1973. Shallow structure and geologic development of the southern Red Sea, *Geol. Soc. Am. Bull.*, **84,** (12), 3827–3848.

Schouten, J. A., 1971. A fundamental analysis of magnetic anomalies over oceanic ridges, *Mar. Geophys. Res.*, **1,** (2), 111–144.

Schouten, H., 1974. Magnetic anomalies over fracture zones in the lower magnetic latitudes of the central North Atlantic, *Trans. Am. geophys. Un.*, **55,** (4), p.232 (abstract).

Schouten, H. & McCamy, K., 1972. Filtering marine magnetic anomalies, *J. geophys. Res.*, **77,** 7089–7099.

Sykes, L. R., 1968. Seismological evidence for transform faults, sea-floor spreading and continental drift, *The history of the Earth's crust*, 120–150, ed. R. A. Phinney, Princeton University Press.

Tramontini, C. & Davies, D., 1969. A seismic refraction survey in the Red Sea, *Geophys. J. R. astr. Soc.*, **17,** 225–241.

Turcotte, D. L., 1974. Are transform faults thermal contraction cracks?, *J. geophys. Res.*, **79,** (17), 2573–2577.

Vine, F. J., 1966. Spreading of the ocean floor: new evidence, *Science*, **154,** 1405–1415.

Vine, F. J. & Matthews, D. H., 1963. Magnetic anomalies over ocean ridges, *Nature*, **199,** 947–949.

Vogt, P. R., Anderson, C. N. & Bracey, D. R., 1971. Mesozoic magnetic anomalies, sea-floor spreading and geomegnetic reversals in the southwestern North Atlantic, *J. geophys. Res.*, **76,** 4796–4823.

Whitmarsh, R. B., Weser, O. E., Ross, D. A. *et al.*, 1974. *Initial Reports of the Deep Sea Drilling Project*, Volume **23,** Washington (U.S. Government Printing Office), 1180 pp.